Supporting Information

Savage et al. 10.1073/pnas.1012194108

SI Text

Resistance per Path Length. Whole-plant resistance, Z_{plant}, is the inverse of plant conductance, κ_{plant}, given by Eq. **6** in the main text. The whole-plant resistance is calculated to be

$$Z_{plant} = \left(\frac{Z_N}{n_{ext}^N}\right)\frac{\left[\left(\frac{l_{TOT}}{l_N}\right)\left(n_{ext}^b - 1\right) + 1\right]^{\left(\frac{b-p}{b}\right)} - 1}{n_{ext}^{b-p} - 1},$$

where $Z_N = (1/N_{\text{int},N}^{\text{seg}})(8\mu l_N/\pi r_{\text{int},N}^4)$ is the total resistance for laminar flow through all conduits in a terminal twig, which is invariant by principle v from the main text. The total path length from stem to terminal twig for the plant is $l_{\text{TOT}} = l_N(n_{\text{ext}}^{b(N+1)} - 1)/(n_{\text{ext}}^b - 1)$. Our expression for whole-plant resistance separates the dependence on the number of terminal twigs and girth of the tree given by Z_N/n_{ext}^N, from the dependence on path length (l_{TOT}/l_N) given by the remainder of the expression. As plants increase in height and total path length $l_{\text{TOT}}/l_N >> 1$, there are two possibilities: (i) If $b - p > 0$, the resistance per path length will increase with path length, l_{TOT}, or (ii) if $b - p < 0$, the total resistance is Z_N/n_{ext}^N, and the resistance per path length is independent of path length l_{TOT}. When $b - p = 0$, l'Hospital's rule requires that resistance depends weakly on path length [$\sim\ln(l_{\text{TOT}})$].

Consequently, minimizing the resistance per path length, analogous to the calculation in the WBE model, demands that $b - p \geq 0$. Minimizing taper relative to this constraint leads to $b = p = 1/3$. This result emphasizes the importance of $p = 1/3$ as a transition point. For allometrically optimal plants, our prediction of $p = 1/3$ differs from the WBE prediction of 1/6 for taper, obtained by holding the conduit frequency constant and not including the packing rule (1, 2).

It is important to emphasize, as in the discussion following Eq. **6** of the main text, that for realistic size ranges across plants, the resistance per path length may still increase significantly as path length increases and may differ dramatically from the asymptotic value. Fig. S1*A* shows that when the taper exponent $p \geq 1/3$ the remainder term of the resistance (dependence on path length) appears to quickly approach an asymptote. In contrast, this is not the case when $p < 1/3$. However, this interpretation is slightly misleading because of the range of resistance considered. For example, by restricting the scale of resistance (Fig. S1*B*) and focusing only on the cases where the taper exponent $p \geq 1/3$, it is evident that resistance per path length does still increase when $p = 1/3$, although at a slower rate than for $p < 1/3$. This result is because for $p = 1/3$ the resistance per path length is predicted to change logarithmically with path length and will not appear constant until trees are many orders of magnitude larger than the tallest trees.

Axial and Radial Taper Data. Our model is designed to describe changes in conduit radii across levels k—proceeding axially, from base to twig through the tree. However, variation in conduit radii also occurs *across* growth rings—outer cambium to the pith—radially within a single branch. The packing rule and tapering seem to exhibit similar patterns both across the tree (axially) *and* within branches (radially) (3–7), reflecting the fact that the inner xylem of a large branch originated when the branch was a narrow terminal twig. This correspondence has been previously used by others to increase the amount of data for regression to perform tests of the WBE model predictions, even though the WBE and our model both effectively ignore variation in conduit radii within branches (radial) (3–7). Because of our extensive data within single trees as well as within and across species, we are able to calculate scaling exponents both for axial measurements, the most direct test of our and the WBE model, and for radial and axial measurements combined, linking our results most directly to previous studies. As shown in Table 1, the measured scaling exponents are in good agreement with each other (axial compared with axial plus radial) and with the predictions of our model.

1. West GB, Brown JH, Enquist BJ (1999) A general model for the structure and allometry of plant vascular systems. *Nature* 400:664–667.
2. West GB, Brown JH, Enquist BJ (1997) A general model for the origin of allometric scaling laws in biology. *Science* 276:122–126.
3. Weitz JS, Ogle K, Horn HS (2006) Ontogenetically stable hydraulic design in woody plants. *Funct Ecol* 20:191–199.
4. Fan ZX, Cao KF, Becker P (2009) Axial and radial variations in xylem anatomy of angiosperm and conifer trees in Yunnan, China. *IAWA J* 30:1–13.
5. Coomes DA, Heathcote S, Godfrey ER, Shepherd JJ, Sack L (2008) Scaling of xylem vessels and veins within the leaves of oak species. *Biol Lett* 4:302–306.
6. Coomes DA, Jenkins KL, Cole LES (2007) Scaling of tree vascular transport systems along gradients of nutrient supply and altitude. *Biol Lett* 3:86–89.
7. Russo SE, Wiser SK, Coomes DA (2007) Growth-size scaling relationships of woody plant species differ from predictions of the Metabolic Ecology Model. *Ecol Lett* 10:889–901.

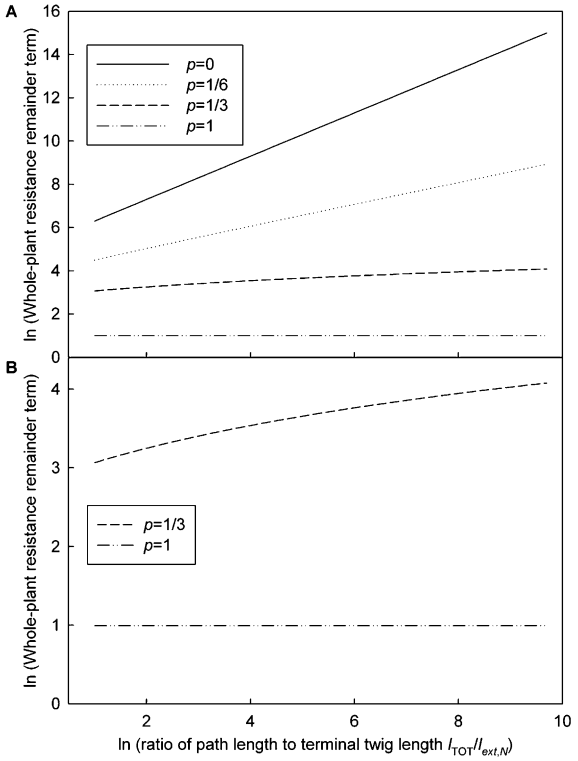

Fig. S1. (*A*) Plots of the remainder term of the resistance, capturing the dependence on total path length, vs. the ratio of total path length to the terminal twig length for realistic plant sizes. For these plots we used a branching ratio of $n_{ext} = 2$ and a terminal twig length of 5 mm and assumed that the total path length for plants ranged from 1 cm, a small seedling, to 80 m, the approximate height of the tallest tree on earth. For values of $p < 1/3$ the remainder term for the resistance increases without bound. For values of $p \geq 1/3$ the remainder term for the resistance approaches an asymptotic limit and appears to be constant as a function of path length. (*B*) Plots of the remainder term of the resistance, capturing the dependence on total path length, vs. the ratio of total path length to the terminal twig length. Here, we have restricted the plot to values of $p = 1/3$ and $p = 1$ so that it is clear that the remainder term for the resistance continues to increase substantially with path length, not reaching its asymptote until the path is much longer than for the tallest trees. Consequently, it is not accurate to claim that resistance is truly independent of path length even for taper exponents of $p \geq 1/3$.

Table S1. Predicted scaling exponents for physiological and anatomical variables of whole-plant and base properties as a function of plant mass (*M*) for the West, Brown, and Enquist (WBE) model and our model

Network property	WBE model exponent for plant mass (*M*)	Our model exponent for plant mass (*M*)
Whole plant		
No. of leaves (N_{leaves})	3/4	3/4
No. of branches ($N_{branches}$)	3/4	3/4
Metabolic rate (B)	3/4	3/4
Stem-to-petiole path length (l_{TOT})	1/4	1/4
Total fluid volume	25/24	1
Stem/branch		
Length ($l_{ext,0}$)	1/4	1/4
Radius ($r_{ext,0}$)	3/8	3/8
Area of conductive tissue ($A^{TOT}_{int,0}$)	7/8	3/4
Active conducting conduit area-to-nonconducting area ratio	1/8	0
No. of conduits ($N_{int,0}$)	3/4	1/2
Conduit radius ($r_{int,0}$)	1/16	1/8
Fluid velocity (u_0)	−1/8	0
Conductivity (K_0)	1	1
Leaf-specific conductivity (K_0/N_{leaves})	1/4	1/4
Pressure gradient ($(P_1 - P_0)/l_0$)	−1/4	−1/4
Resistance ($Z_0/N_{int,0}$)	−3/4	−3/4

The predictions derived from the external network (identical between models) are unchanged, whereas predictions that depend on the internal conduit network differ. For these predictions we ignore finite-size effects, which alter these scaling exponents depending on the size ranges of the plants considered. See also discussion connected to Fig. 2 in main text.

Table S2. Sources for literature data

Network property	Taxa	Reference
Packing	Angiosperms/conifers	(1)
Taper	*Betula pendula*	(2)
	Fraxinus americana	(3)
	Larix decidua	(4)
	Nothofagus solandi, *Picea abies*, *Pinus sylvestris*	(5)
	Tsuga canadensis	(6)
Velocity	*Pseudotsuga menziesii*	(7)
	Eucalyptus regnans	(8)
	Citrus sinensis, Cupressus sempervirens, Eucalyptus camaldulensis, Malus domestica, Persea americana, Pinus halepensis, Quercus calliprinos, Quercus ithaburensis	(9)
	Acer saccharum	(10)
	Liriodendron tulipifera	(11)
Sap flux	Angiosperms	(12)
	Angiosperms	(13)
	Conifers	(14)
	Angiosperms	(15)
	Angiosperms	(16)
	Angiosperms	(17)
	Conifers	(18)
	Conifers	(19)
	Conifers	(20)
	Angiosperms	(21)
	Angiosperms	(22)
	Conifers	(23)
	Angiosperms	(24)
	Angiosperms	(25)
	Conifers	(26)
	Angiosperms	(27)
	Conifers	(28)
	Angiosperms	(29)
	Conifers	(30)
	Angiosperms	(31)
	Angiosperms	(32)
	Angiosperms	(33)
	Angiosperms	(34)
	Angiosperms	(35)
	Angiosperms	(36)
Hydraulic conductivity	*Acer rubrum, Acer saccharum, P. sylvestris, Pinus banksiana*	(37)
Leaf-specific hydraulic conductivity	*Tsuga canadensis*	(6)
	Ficus glabrata	(38)
	Thuja occidentalis	(39)
	A. saccharum, Schefflera morototoni, T. occidentalis	(40)
	Sequoiadendron giganteum, *Sequoia sempervirens*	(41)

1. Sperry JS, Meinzer FC, McCulloh KA (2008) Safety and efficiency conflicts in hydraulic architecture: Scaling from tissues to trees. *Plant Cell Environ* 31:632–645.
2. Sellin A, Rohejarv A, Rahi M (2008) Distribution of vessel size, vessel density and xylem conducting efficiency within a crown of silver birch (Betula pendula). *Trees Struct Funct* 22: 205–216.
3. Weitz JS, Ogle K, Horn HS (2006) Ontogenetically stable hydraulic design in woody plants. *Funct Ecol* 20:191–199.
4. Anfodillo T, Carraro V, Carrer M, Fior C, Rossi S (2006) Convergent tapering of xylem conduits in different woody species. *New Phytol* 169:279–290.
5. Coomes DA, Jenkins KL, Cole LE (2007) Scaling of tree vascular transport systems along gradients of nutrient supply and altitude. *Biol Lett* 3:86–89.
6. Ewers FW, Zimmermann MH (1984) The hydraulic architecture of eastern hemlock (Tsuga-canadensis). *Can J Bot* 62:940–946.
7. Meinzer FC, et al. (2006) Dynamics of water transport and storage in conifers studied with deuterium and heat tracing techniques. *Plant Cell Environ* 29:105–114.
8. Vertessy RA, Hatton TJ, Reece P, O'Sullivan SK, Benyon RG (1997) Estimating stand water use of large mountain ash trees and validation of the sap flow measurement technique. *Tree Physiol* 17:747–756.
9. Cohen Y, Cohen S, Cantuarias-Aviles T, Schiller G (2008) Variations in the radial gradient of sap velocity in trunks of forest and fruit trees. *Plant Soil* 305:49–59.
10. Dragoni D, Caylor KK, Schmid HP (2009) Decoupling structural and environmental determinants of sap velocity Part II. Observational application. *Agric For Meteorol* 149:570–581.
11. Wullschleger SD, King AW (2000) Radial variation in sap velocity as a function of stem diameter and sapwood thickness in yellow-poplar trees. *Tree Physiol* 20:511–518.
12. Meinzer FC (2003) Functional convergence in plant responses to the environment. *Oecologia* 134:1–11.
13. Dierick D, Holscher D (2009) Species-specific tree water use characteristics in reforestation stands in the Philippines. *Agric For Meteorol* 149:1317–1326.
14. Cermak J, Kucera J, Nadezhdina N (2004) Sap flow measurements with some thermodynamic methods, flow integration within trees and scaling up from sample trees to entire forest stands. *Trees Struct Funct* 18:529–546.
15. Jordan CF, Kline JR (1977) Transpiration of trees in a tropical rainforest. *J Appl Ecol* 14:853–860.

16. Kline JR, Martin R, Jordan CF, Koranda JJ (1970) Measurement of transpiration in tropical trees with tritiated water. *Ecology* 51:1068–1073.
17. Dye PJ, Olbrich BW, Calder IR (1992) A comparison of the heat pulse method and deuterium tracing method for measuring transpiration from Eucalyptus-grandis trees. *J Exp Bot* 43: 337–343.
18. Kline JR, Reed KL, Waring RH, Stewart ML (1976) Field measurement of transpiration in Douglas-fir. *J Appl Ecol* 13:273–283.
19. Swanson RH (1972) Water transpired by trees is indicated by heat pulse velocity. *Agric Meteorol* 10:277.
20. Schulze ED, et al. (1985) Canopy transpiration and water fluxes in the xylem of the trunk of Larix and Picea trees - a comparison of xylem flow, porometer and cuvette measurements. *Oecologia* 66:475–483.
21. Sakuratani T (1981) A heat balance method for measuring water flux in the stem of intact plants. *J Agr Met* 37:9–17.
22. Olbrich BW (1991) The verification of the heat pulse velocity technique for estimating sap flow in Eucalyptus-grandis. *Can J Res* 21:836–841.
23. Luvall JC, Murphy CE (1982) Evaluation of the tritiated-water method for measurement of transpiration in young Pinus-taeda L. *For Sci* 28:5–16.
24. Cermak J, Palat M, Penka M (1976) Transpiration flow-rate in a full-grown tree of Prunus-avium-L estimated by method of heat balance in connection with some meteorological factors. *Biol Plant* 18:111–118.
25. Sakuratani T (1979) Apparant thermal conductivity of rice stems in relation to transpiration stream. *J Agr Met* 34:177–187.
26. Decker JP, Skau CM (1964) Simultaneous studies of transpiration rate + sap velocity in trees. *Plant Physiol* 39:213–215.
27. Hinckley TM, et al. (1994) Water flux in a hybrid poplar stand. *Tree Physiol* 14:1005–1018.
28. Cienciala E, Lindroth A, Cermak J, Hallgren JE, Kucera J (1992) Assessment of transpiration estimates for Picea-abies trees during a growing-season. *Trees Struct Funct* 6:121–127.
29. Calder IR, Narayanswamy MN, Srinivasalu NV, Darling WG, Lardner AJ (1986) Investigation into the use of deuterium as a tracer for measuring transpiration from eucalypts. *J Hydrol (Amst)* 84:345–351.
30. Cohen Y, Kelliher FM, Black TA (1985) Determination of sap flow in douglas fir trees using the heat pulse technique. *Can J Res* 15:422–428.
31. Green SR, Clothier BE (1988) Water-use of kiwifruit vines and apple-trees by the heat-pulse technique. *J Exp Bot* 39:115–123.
32. Steinberg SL, Vanbavel CHM, McFarland MJ (1990) Improved sap flow gauge for woody and herbaceous plants. *Agron J* 82:851–854.
33. Hatton TJ, Moore SJ, Reece PH (1995) Estimating stand transpiration in a Eucalyptus populnea woodland with the heat pulse method: Measurement errors and sampling strategies. *Tree Physiol* 15:219–227.
34. Heilman JL, Ham JM (1990) Measurement of mass-flow rate of sap in Ligustrum-japonicum. *HortScience* 25:465–467.
35. Valancogne C, Nasr Z (1989) Measuring sap flow in the stem of small trees by a heat-balance method. *HortScience* 24:383–385.
36. Doley D, Grieve BJ (1966) Measurement of sap flow in a eucalypt by thermo-electric methods. *Aust For Res* 2:3–27.
37. Mencuccini M (2002) Hydraulic constraints in the functional scaling of trees. *Tree Physiol* 22:553–565.
38. Patino S, Tyree MT, Herre EA (1995) Comparison of hydraulic architecture of woody-plants of differing phylogeny and growth form with special reference to freestanding and hemi-epiphytic Ficus species from Panama. *New Phytol* 129:125–134.
39. Tyree MT, Graham MED, Cooper KE, Bazos LJ (1983) The hydraulic architecture of Thuja-occidentalis. *Can J Bot* 61:2105–2111.
40. Tyree MT, Snyderman DA, Wilmot TR, Machado JL (1991) Water relations and hydraulic architecture of a tropical tree (Schefflera-morototoni) - data, models, and a comparison with 2 temperate species (Acer-saccharum and Thuja-occidentalis). *Plant Physiol* 96:1105–1113.
41. Ambrose AR, Sillett SC, Dawson TE (2009) Effects of tree height on branch hydraulics, leaf structure and gas exchange in California redwoods. *Plant Cell Environ* 32:743–757.

Table S3. Observed values for intraspecific scaling exponents (and 95% confidence intervals and r^2 values) as a function of branch radius ($r_{ext,k}$) for empirical data related to internal network structure measured across three contrasting species (n = 3 trees for all values for oak and maples; n = 2 trees for all values for pine except number of conduits with n = 3)

Network property	Our model predicted exponent for $r_{ext,k}$	Oak observed exponent for $r_{ext,k}$	Maple observed exponent for $r_{ext,k}$	Pine observed exponent for $r_{ext,k}$
No. of conduits in a branch segment ($N^{seg}_{int,k}$)	4/3 = 1.33...	1.12 (1.01, 1.24; r^2 = 0.51)	1.08 (0.99, 1.18; r^2 = 0.36)	1.45 (1.40, 1.49; r^2 = 0.95)
Conducting-to-nonconducting ratio	0	0.56 (0.49, 0.63; r^2 = 0.30)	−0.42 (−0.47, −0.38; r^2 = 0.04)	0.33 (0.28, 0.40; r^2 = 0.06)
Conduit radius (taper, $r_{int,k}$)	1/3 = 0.33...	0.46 (0.42, 0.50; r^2 = 0.63)	0.23 (0.21, 0.25; r^2 = 0.36)	0.20 (0.17, 0.22; r^2 = 0.55)
Packing rule (no. frequency of conduits vs. conduit radius, $r_{int,k}$, not branch radius, $r_{ext,k}$)	−2	−1.44 (−1.55, −1.33; r^2 = 0.72)	−2.73 (−2.90, −2.57; r^2 = 0.68)	−1.67 (−1.78, −1.56; r^2 = 0.86)

Regression exponents were calculated using RMA regression within (S)MATR software using both radial and axial xylem data. Performing regressions on individual trees within the same species leads to very similar results.